ARRANGEMENT OF VORTEX LATTICES

ON SUBSONIC WINGS*

Fred R. DeJarnette
North Carolina State University

SUMMARY

A new method is developed for solving the lifting-surface equation for thin wings. The solution requires the downwash equation to be in the form of Cauchy integrals which can be interpreted as a vortex lattice with the positions of the vortices and control points dictated by the finite sum used to approximate the integrals involved. Lan's continuous loading method is employed for the chordwise integral since it properly accounts for the leading-edge singularity, Cauchy singularity, and Kutta condition. Unlike Lan, the spanwise loading is also continuous and the Cauchy singularity in the spanwise integral is also properly accounted for by using the midpoint trapezoidal rule and the theory of Chebychev polynomials. This technique yields the exact classical solution to Prandtl's lifting-line equation. The solution to the lifting-surface equation for rectangular wings was found to compare well with other continuous loading methods, but with much smaller computational times, and it converges faster than other vortex lattice methods.

INTRODUCTION

The vortex lattice method has proven to be a useful technique for calculating the aerodynamic characteristics of complete configurations as well as wings. In the conventional vortex lattice method (VLM), the planform is divided into a number of elemental panels, and a horseshoe vortex is placed at the local quarter-chord of each panel. The boundary condition is satisfied at the local three-quarter chord of each elemental panel (called control points) by requiring the flow to be tangent to the surface there. The strengths of the horseshoe vortices are determined by solving the matrix equation formed from the tangent-flow boundary conditions. Then, the aerodynamic characteristics are calculated by summing the results from each elemental panel. A complete description of the conventional vortex lattice method is given by Margason and Lamar in reference 1.

Although reasonable results are obtained by the conventional VLM, Lan (ref. 2) listed the following deficiencies: 1) The method used to compute the induced drag implies that the leading-edge thrust is distributed over the chord

---

instead of being concentrated at the leading edge. 2) The predicted pressure distribution is not accurate near the leading edge. 3) The convergence of solutions is slow with respect to the number of panels used. In addition, the Kutta condition is not explicitly satisfied. Hough (ref. 3) found some improvement by using a 1/4 lattice width inset at the wing tips.

Lan (ref. 2) developed an ingenious method for thin, two-dimensional airfoils by using the midpoint trapezoidal rule and the theory of Chebychev polynomials to reduce the downwash integral to a finite sum. This method gives the exact lift, pitching moment, leading-edge suction, and pressure difference at a finite number of points; and the Kutta condition is satisfied at the trailing edge. A more detailed description is given below. Lan also developed a quasi-vortex lattice method for finite wings by using his two-dimensional method for the continuous chordwise vortex distribution but a stepwise constant vortex distribution in the spanwise direction. The results showed an improvement over those calculated by the conventional vortex lattice method.

This paper develops a new vortex lattice method which uses Lan's continuous chordwise vortex distribution but, unlike Lan, a continuous spanwise vortex distribution also. Although the vortex distributions are continuous, the method is easily interpreted as a vortex lattice method in which the arrangement of horseshoe vortices and control points are determined from the finite sum used to approximate the downwash integral of lifting-surface theory. In order to understand the development of the present method, Lan's two-dimensional theory is reviewed first, and then the present method is applied to Prandtl's lifting-line theory before developing the method for lifting-surface theory.

SYMBOLS

A   aspect ratio

b   wing span

c   wing chord

c_ℓ sectional lift coefficient

c_m sectional moment coefficient about leading edge

c_t sectional leading-edge thrust coefficient

C_{D_i} far-field induced drag coefficient

$C_{D_{ii}}$ near-field induced drag coefficient

C_L wing lift coefficient

302

C_{L_α} lift-curve slope, per radian except when noted otherwise

C_M wing pitching moment coefficient about leading edge

C_{M_α} pitching-moment curve slope, per radian

C_S leading-edge suction parameter

C_T wing leading-edge thrust coefficient

e far-field spanwise efficiency factor, $C_L{}^2/C_{D_i} \, \pi \, A$

e_{nf} near-field efficiency factor, $C_L{}^2/C_{D_{ii}} \, \pi \, A$

$K_{ijk\ell}$ parameter defined by eq. (26)

M number of trailing vortices over whole wing span

$M-1$ number of spanwise control points over whole span

n summational integer

N number of chordwise vortices and control points

NLR   National Aerospace Laboratory, Netherlands

S wing planform area

VLM   vortex lattice method

V_∞ freestream velocity

w downwash velocity, referred to V_∞ and positive upwards

x chordwise coordinate measured from leading edge in direction of V_∞

x_{ac}, X_{ac} sectional and wing aerodynamic center locations, respectively

y spanwise coordinate, positive to the right

z_c vertical coordinate of mean camber line

α angle of attack

γ nondimensional circulation per unit chord

Γ circulation

ΔC_p difference between lower and upper pressure coefficients ($\Delta C_p = 2\gamma$)

θ transformed chordwise coordinate, see eq. (2)

ϕ transformed spanwise coordinate, see eq. (12)

Subscripts:

i   chordwise control point, see eq. (7)

j   spanwise control point, see eq. (15)

k   chordwise vortex position, see eq. (6)

ℓ spanwise trailing vortex position, see eq. (14)

p   evaluated at spanwise position $\phi_p = p\pi/M$

LAN'S TWO-DIMENSIONAL THEORY

For thin airfoils, the downwash equation is

$$w_i = -\frac{1}{2\pi} \int_0^c \frac{\gamma(x_1)\ dx_1}{x_i - x_1} \tag{1}$$

The integral on the right side is of the Cauchy type. Transform the x coordinate by

$$x/c = (1 - \cos\theta)/2 \tag{2}$$

and use the following result from airfoil theory (ref. 4)

$$\int_0^\pi \frac{d\theta_1}{\cos\theta_1 - \cos\theta} = 0 \tag{3}$$

to write eq. (1) as

$$w_i = -\frac{1}{2\pi} \int_0^\pi \frac{\gamma(\theta_1) \sin \theta_1 \, d\theta_1}{\cos \theta_1 - \cos \theta} = -\frac{1}{2\pi} \int_0^\pi \frac{[\gamma(\theta_1) \sin \theta_1 - \gamma(\theta) \sin \theta] d\theta_1}{\cos \theta_1 - \cos \theta} \qquad (4)$$

Lan (ref. 2) used the theory of Chebychev polynomials to show that

$$\sum_{k=1}^{N} \frac{1}{\cos \theta_k - \cos \theta_i} = \begin{cases} -N^2 & \text{for} \quad i = 0 \\ 0 & \text{for} \quad i \neq 0, N \\ N^2 & \text{for} \quad i = N \end{cases} \qquad (5)$$

when the vortex positions are

$$\theta_k = \frac{(2k-1)\pi}{2N} \quad , \quad k = 1, \ldots, N \qquad (6)$$

and the control points are located at

$$\theta_i = \frac{i\pi}{N} \quad , \quad i = 0, 1, \ldots, N \qquad (7)$$

Then the integral in eq. (4) can be reduced to a finite sum by using the mid-point trapezoidal rule (ref. 5) and eq. (5) to obtain

$$w_i = -\frac{1}{2\pi} \frac{\pi}{N} \sum_{k=1}^{N} \frac{\gamma_k \sin \theta_k - \gamma_i \sin \theta_i}{\cos \theta_k - \cos \theta_i}$$

$$= -\frac{1}{2N} \sum_{k=1}^{N} \frac{\gamma_k \sin \theta_k}{\cos \theta_k - \cos \theta_i} + \begin{cases} -\frac{N}{2} \lim_{\theta \to 0} \gamma(\theta) \sin \theta & , \quad i = 0 \\ 0 & , \quad i \neq 0, N \\ \frac{N}{2} \lim_{\theta \to \pi} \gamma(\theta) \sin \theta & , \quad i = N \end{cases} \qquad (8)$$

However,

$$\lim_{\theta \to 0} \gamma(\theta) \sin \theta = 4 C_s \qquad (9)$$

where C_s is the leading-edge suction parameter and since the Kutta condition requires that $\gamma(\pi) = 0$,

$$\lim_{\theta \to \pi} \gamma(\theta) \sin \theta = 0 \qquad (10)$$

Unlike the conventional vortex lattice method, the Cauchy singularity, leading-edge square-root singularity and the Kutta condition are properly accounted for in this method. Equation (8) can be solved with $i \neq 0$ to obtain

305

the N values of γ_k, and then the leading-edge suction parameter can be computed by using eq. (8) with i = 0 (control point at the leading edge). Figure 1 illustrates the positions of the vortices and control points by the "semicircle method" for N = 2. With only one vortex (N = 1), the exact lift and leading-edge suction are obtained, and the Kutta condition is satisfied. With two or more vortices the exact pitching moment is obtained in addition to the above properties and the calculated values of γ_k are exact. It can be shown that the remarkable accuracy of this method is due to eq. (5), which is similar to the integral result given by eq. (3) and used in exact thin airfoil theory.

PRANDTL'S LIFTING-LINE THEORY

Before attacking the lifting-surface equation, the present method will be developed for Prandtl's lifting-line equation to compare the spanwise lift distribution with the classical solution (ref. 4). The lifting-line equation is given by ref. 6,

$$\Gamma = \pi \, V_\infty \, c \left[\alpha - \frac{1}{4\pi \, V_\infty} \int_{-b/2}^{b/2} \frac{d\Gamma}{dy_1} \frac{dy_1}{(y - y_1)} \right] \tag{11}$$

This equation also has a Cauchy integral on the right side, and thus Lan's airfoil technique is applicable. Transform the spanwise coordinate by

$$y = - \frac{b}{2} \cos \phi \tag{12}$$

and replace the downwash integral in eq. (11) with the midpoint trapezoidal-rule summation to get

$$w_j = - \frac{1}{4\pi \, V_\infty} \int_{-b/2}^{b/2} \frac{d\Gamma}{dy_1} \frac{dy_1}{(y_j - y_1)} \simeq - \frac{1}{4\pi \, V_\infty} \frac{\pi}{M} \frac{2}{b} \sum_{\ell=1}^{M} \frac{(d\Gamma/d\phi_1)_\ell}{\cos \phi_\ell - \cos \phi_j} \tag{13}$$

This equation represents the downwash due to M trailing vortices of strength $-(d\Gamma/d\phi_1)_\ell \, (\pi/M)$ located at

$$\phi_\ell = \frac{(2\ell - 1)\pi}{2M} \quad , \quad \ell = 1, \ldots, M \tag{14}$$

with control points located at

$$\phi_j = \frac{j\pi}{M} \quad , \quad j = 1, \ldots, M-1 \tag{15}$$

306

Now the conventional vortex lattice arrangement is shown in figure 2*, whereas the present arrangement is shown in figure 3. Note in particular that the tip vortices extend to the wing tip in the conventional method, whereas eq. (14) determines them to be inset (see fig. 3), which agrees with Hough's results (ref. 3).

Since $(d\Gamma/d\phi_1)_\ell$ is needed in eq. (13), it is convenient to represent the circulation by Multhopp's interpolation formula

$$\Gamma(\phi) = \frac{2}{M} \sum_{p=1}^{M-1} \Gamma_p \sum_{n=1}^{M-1} \sin n\phi_p \sin n\phi \tag{16}$$

where

$$\phi_p = \frac{p\pi}{M} \quad , \quad p = 1, \ldots, M-1 \tag{17}$$

Equation (16) is based on the following orthogonality property (ref. 7)

$$\frac{\pi}{M} \sum_{n=1}^{M-1} \sin n\phi_p \sin n\phi_j = \begin{cases} \frac{\pi}{2} & \text{for} \quad p = j \\ \\ 0 & \text{for} \quad p \neq j \end{cases} \tag{18}$$

Substitute eq. (16) into eq. (13) and then the downwash becomes

$$w_j \simeq - \frac{1}{V_\infty M^2 b} \sum_{\ell=1}^{M} \sum_{p=1}^{M-1} \Gamma_p \sum_{n=1}^{M-1} \frac{\sin n\phi_p \, n \cos n\phi_\ell}{\cos \phi_\ell - \cos \phi_j} \tag{19}$$

However, this result can be simplified by using eq. (5) to derive the important summation below

$$\frac{\pi}{M} \sum_{\ell=1}^{M} \frac{\cos n\phi_\ell}{\cos \phi_\ell - \cos \phi_j} = \frac{\pi \sin n\phi_j}{\sin \phi_j} \tag{20}$$

This equation is similar to the following integral result used in thin airfoil and lifting-line analyses (ref. 4)

$$\int_0^\pi \frac{\cos n\phi_1 \, d\phi_1}{\cos \phi_1 - \cos \phi} = \frac{\pi \sin n\phi}{\sin \phi} \tag{21}$$

When eq. (20) is used in eq. (19), the downwash reduces to

---

* In some conventional techniques the spanwise length of each vortex is uniform, but it is reported to have little effect on the results.

$$w_j \simeq -\frac{1}{V_\infty M b} \sum_{p=1}^{M-1} \Gamma_p \sum_{n=1}^{M-1} \frac{\sin n\phi_p \, n \sin n\phi_j}{\sin \phi_j} \qquad (22)$$

Finally, substitute eq. (22) for the downwash in eq. (11) and apply the resulting equation at the spanwise locations ϕ_j ($j = 1, \ldots, M-1$) to obtain a matrix equation for the $(M-1)$ values of Γ_p. Then, the lift, pitching moment, and induced drag can be calculated by reducing the spanwise integrals to a finite sum through the midpoint trapezoidal rule. However, the midpoint trapezoidal rule gives exactly the same result for the spanwise integrals as the integral itself when eq. (16) is used for Γ. To prove this assertion, consider the spanwise integral for the lift. Using eq. (16), the exact integral result is

$$C_L \, V_\infty \frac{S}{b} = \frac{2}{b} \int_{-b/2}^{b/2} \Gamma \, dy = \frac{\pi}{M} \sum_{p=1}^{M-1} \Gamma_p \sin \phi_p$$

whereas the midpoint trapezoidal rule gives

$$\frac{2}{b} \int_{-b/2}^{b/2} \Gamma \, dy \simeq \frac{2\pi}{M^2} \sum_{\ell=1}^{M} \sum_{p=1}^{M-1} \Gamma_p \sum_{n=1}^{M-1} \sin n\phi_p \, \sin n\phi_\ell \, \sin \phi_\ell = \frac{\pi}{M} \sum_{p=1}^{M-1} \Gamma_p \sin \phi_p$$

which is the same as the exact integral result above. In obtaining this last result, the following orthogonality property was applied

$$\frac{\pi}{M} \sum_{\ell=1}^{M} \sin n\phi_\ell \, \sin \phi_\ell = \begin{cases} \dfrac{\pi}{2} & \text{for} \quad n = 1 \\[2mm] 0 & \text{for} \quad n \neq 1 \end{cases}$$

The integrals for the induced drag are handled in a similar fashion.

The remarkable feature of the present method is that the results are identical to the classical solution of Prandtl's lifting-line equation when a finite number of terms is used in the Fourier series for Γ (ref. 4). The success of the present method is attributed to the location of the spanwise vortices and control points, the summational result of eq. (20), and the accuracy of the midpoint trapezoidal rule for the spanwise integrals.

Figure 4 illustrates the convergence of this method compared with the conventional VLM for C_{L_α} of rectangular and elliptical planforms with an aspect ratio of 2π. Prandtl's lifting-line theory requires trailing vortices and spanwise control points, but no chordwise control points are needed because the theory assumes the downwash is constant in the chordwise direction. Therefore, the control points are placed on the "bound" vortex for both methods. In this way, the accuracy of the spanwise vortex arrangement can be tested without the influence of the location of chordwise control points. Figure 4 shows that the

conventional VLM converges slowly and C_{L_α} does not appear to approach the correct limit when the curve is extrapolated to an infinite number of trailing vortices, $M \to \infty$ $(1/M \to 0)$. On the other hand, the present method converges very quickly and approaches the correct limit. As in the classical solutions, only one horseshoe vortex $(M=2)$ is needed to obtain the exact C_{L_α} for the elliptical planform in Prandtl's lifting-line theory. Figure 5 illustrates the effect of the number of trailing vortices on the spanwise efficiency factor used in the induced drag. Here again, the conventional VLM converges slowly and does not appear to approach the correct limit, whereas the present method converges quickly and approaches the correct limit.

LIFTING-SURFACE THEORY

For simplicity, the present method is developed here for rectangular wings. The downwash equation from lifting-surface theory is usually given by one of the two following integrals (ref. 6)

$$w(x,y) = \frac{1}{4\pi} \int\int_S \frac{\gamma(x_1, y_1)}{(y - y_1)^2} \left[1 + \frac{(x - x_1)}{\sqrt{(x - x_1)^2 + (y - y_1)^2}} \right] dx_1 \, dy_1 \qquad (23)$$

or

$$w(x,y) = -\frac{1}{4\pi} \int\int_S \frac{\partial\gamma}{\partial y_1} \frac{1}{(y - y_1)} \left[1 + \frac{\sqrt{(x - x_1)^2 + (y - y_1)^2}}{(x - x_1)} \right] dx_1 \, dy_1 \qquad (24)$$

Equation (23) contains the Mangler-type integral, and therefore, is not suitable for the present method. Equation (24), however, contains Cauchy-type integrals and is therefore in the form to apply a combination of Lan's two-dimensional method for the chordwise integration and the lifting-line method developed above for the spanwise integration. Note that the integrand of eq. (24) represents the downwash at (x,y) due to half of a horseshoe vortex as shown below.
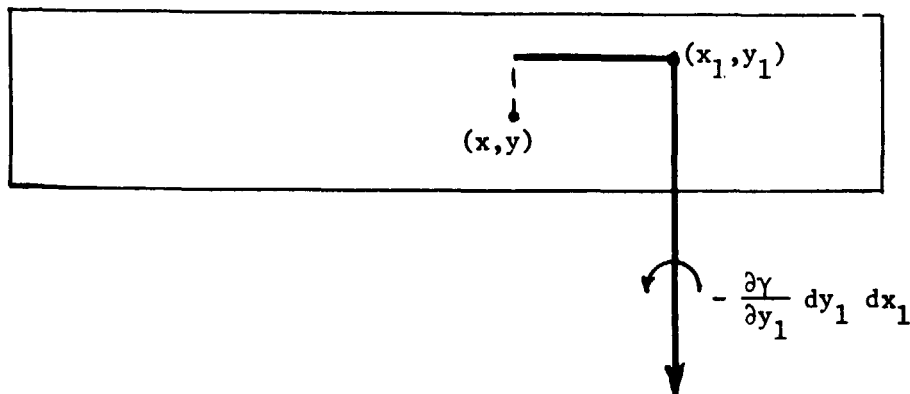
With $y = -b \cos \phi/2$ and $x/c = (1 - \cos \theta)/2$, replace both integrals in eq. (24) with the midpoint trapezoidal-rule sum to get

$$w_{i,j} \simeq -\frac{1}{4\pi} \frac{\pi}{M} \frac{\pi}{N} \frac{c}{b} \sum_{\ell=1}^{M} \sum_{k=1}^{N} \left(\frac{\partial\gamma}{\partial\phi_1}\right)_{k,\ell} \frac{K_{ijk\ell} \sin \theta_k}{(\cos \phi_\ell - \cos \phi_j)} + \begin{cases} -2NC_{S_j} & , i = 0 \\ \\ 0 & , i \neq 0 \end{cases} \qquad (25)$$

where

$$K_{ijk\ell} \equiv 1 + \frac{\sqrt{(\cos \theta_k - \cos \theta_i)^2 + A^2(\cos \phi_\ell - \cos \phi_j)^2}}{\cos \theta_k - \cos \theta_i} \qquad (26)$$

The control points are located at

$$\theta_i = \frac{i\pi}{N} , \ i = 1, \ldots, N \quad \text{(chordwise)} \qquad (27)$$

and

$$\phi_j = \frac{j\pi}{M} , \ j = 1, \ldots, M-1 \quad \text{(spanwise)} \qquad (28)$$

and the "joint" in the horseshoe vortices are located at

$$\theta_k = \frac{(2k - 1)\pi}{2N} , \ k = 1, \ldots, N \quad \text{(chordwise)} \qquad (29)$$

and

$$\phi_\ell = \frac{(2\ell - 1)\pi}{2M} , \ \ell = 1, \ldots, M \quad \text{(spanwise)} \qquad (30)$$

The positions of the horseshoe vortices and the control points are illustrated in figure 6 by the "semicircle method" for two chordwise vortices (N=2) and four trailing vortices (M=4). As in eq. (16), represent the spanwise variation of $\gamma_k(\phi)$, at the chordwise position θ_k, by Multhopp's interpolation formula,

$$\gamma_k(\phi) = \frac{2}{M} \sum_{p=1}^{M-1} \gamma_{p,k} \sum_{n=1}^{M-1} \sin n\phi_p \sin n\phi \qquad (31)$$

where $\gamma_{p,k}$ represents the unknown circulations per unit chord at θ_k and $\phi_p = p\pi/M$. Substitute eq. (31) into eq. (25) to obtain the final form of the downwash as

$$w_{i,j} = \frac{-\pi c}{2bM^2 N} \sum_{\ell=1}^{M} \sum_{k=1}^{N} \sum_{p=1}^{M-1} \gamma_{p,k} \sum_{n=1}^{M-1} \frac{n \sin n\phi_p \cos n\phi_\ell \ K_{ijk\ell} \sin \theta_k}{(\cos \phi_\ell - \cos \phi_j)} + \begin{cases} -2NC_{S_j} & , i = 0 \\ \\ 0 & , i \neq 0 \end{cases} \qquad (32)$$

310

The tangent-flow boundary condition for thin wings requires that

$$w_{i,j} = \left(\frac{\partial z_c}{\partial x}\right)_{i,j} - \alpha \tag{33}$$

where $z_c(x,y)$ is the shape of the mean camber line. The $N(M-1)$ values of $\gamma_{p,k}$ are calculated by solving the matrix equation formed by applying eq. (32) for $i \neq 0$ at the chordwise and spanwise control points given by eqs. (27) and (28). Then after $\gamma_{p,k}$ is calculated, the $(M-1)$ leading-edge suction parameters C_{Sj} can be computed by successively applying eq. (32) with $i = 0$ (control point at the leading edge) at the spanwise positions $j = 1, \ldots, M-1$. Regardless of the number (N) of chordwise vortices used, there is always a control point at the trailing edge which satisfies the Kutta condition, and another control point at the leading edge which gives the leading-edge suction parameter, if desired.

The sectional and wing aerodynamic characteristics may now be calculated by using the midpoint trapezoidal rule to reduce the integrals to finite sums, as shown below (for rectangular wings)

$$(c_\ell)_p = \frac{2\Gamma_p}{c\, V_\infty} = \frac{2}{c} \int_0^c \gamma_p(x_1)\, dx_1 \simeq \frac{\pi}{N} \sum_{k=1}^{N} \gamma_{p,k} \sin \theta_k \tag{34}$$

$$C_L = \int_{-b/2}^{b/2} c_\ell\, c\, dy \Big/ S \simeq \frac{\pi}{2M} \sum_{p=1}^{M-1} (c_\ell)_p \sin \phi_p \tag{35}$$

$$(c_m)_p = - \frac{2}{c^2} \int_0^c \gamma_p(x_1)\, x_1\, dx_1 \simeq - \frac{\pi}{2N} \sum_{k=1}^{N} \gamma_{p,k} (1 - \cos \theta_k) \sin \theta_k \tag{36}$$

$$C_M = \int_{-b/2}^{b/2} c_m\, c^2\, dy \Big/ Sc \simeq \frac{\pi}{2M} \sum_{p=1}^{M-1} (c_m)_p \sin \phi_p \tag{37}$$

$$(x_{ac}/c)_p = - (c_m/c_\ell)_p \tag{38}$$

$$X_{ac}/c = - C_M/C_L \tag{39}$$

$$C_{D_i} = \frac{C_L^2}{\pi A} \sum_{n=1}^{M-1} n \left[\sum_{p=1}^{M-1} \Gamma_p \sin n\phi_p\right]^2 \Big/ \left[\sum_{p=1}^{M-1} \Gamma_p \sin \phi_p\right]^2 \tag{40}$$

$$(c_t)_j = 2\pi \, c_{s_j}^2 \tag{41}$$

$$C_T = \int_{-b/2}^{b/2} c_t \, c \, dy \Big/ S \simeq \frac{\pi}{2M} \sum_{j=1}^{M-1} (c_t)_j \sin \phi_j \tag{42}$$

$$C_{D_{ii}} = C_L \, \alpha - C_T \tag{43}$$

The spanwise loading can be made continuous by eq. (31), and the chordwise loading can also be made cortinuous by fitting C_{s_j} and $\gamma_{j,k}$ to the chordwise loading functions for thin airfoil theory (ref. 4).

RESULTS FOR RECTANGULAR WINGS

For one horseshoe vortex and one control point (N=1, M=2), the present method yields

$$C_{L_\alpha} = \frac{\pi A}{1 + \sqrt{1 + A^2/7}} \quad \text{and} \quad C_{D_i} = \frac{C_L^2}{\pi A}$$

These results give the correct limit as $A \to 0$, but just as Lan found for airfoils, at least two chordwise vortices are needed to get an accurate pitching moment.

Table 1 gives a detailed comparison of the results of the present method with those of several other methods for a flat A = 2 rectangular wing. The methods chosen for comparison are the continuous loading method of the National Aerospace Laboratory of the Netherlands (NLR) presented in ref. 8, Lan's quasi-vortex lattice method (ref. 2), the conventional vortex lattice method of Margason and Lamar (ref. 1), and Wagner's continuous loading method (see ref. 2). In the NLR method (M-1) spanwise loading functions are applied but 8M spanwise integration points are used. Therefore, the results from this method are used as a base for comparison purposes. Table 1 shows that the present method yields more accurate overall aerodynamic characteristics than either the conventional VLM or Lan's quasi-vortex lattices. This table also shows that the spanwise variation of the sectional lift coefficient compares within four significant figures to those of the NLR method. The spanwise variation of the sectional aerodynamic center also compares well except near the wing tip. When the number of chordwise vortices was increased from N = 4 to N = 6 in the present method, these differences decreased considerably. Figure 7 compares the present method with the NLR method for the chordwise loading at midspan on this same A = 2 wing. Again, the results compare quite well.

The computational time required for the results in Table 1 was 22 minutes for the NLR method on a CDC 3300 computer; Lan's method required one minute on

the Honeywell 635 computer; Wagner's method used about three minutes; and
the present method required less than ten seconds on an IBM 370/165. Therefore,
the present method is as economical as the VLM for the same number of vortices,
but it is generally more economical when one considers that a smaller number of
vortices can be used to achieve the same accuracy as the VLM.

The effect of the vortex lattice arrangement on the convergence of the
lift-curve slope is presented in figure 8 and compared with the conventional
VLM for flat rectangular wings with A = 2, 4.5, and 7. This figure illustrates
again the slow convergence of the conventional VLM and the rapid convergence of
the present method. For all three wings, the present method gives good ac-
curacy with only two chordwise vortices, but more spanwise vortices are needed
for the A = 7 wing ($M/2 \simeq 10$) than the A = 4.5 wing ($M/2 \simeq 5$) or A = 2 wing
($M/2 \simeq 2$). Results for the pitching moment, aerodynamic center location, and
induced drag were found to converge even faster than the lift-curve slope,
therefore they are not presented.

The Prandtl-Glauert rule can be easily applied to the present method to
include subsonic compressibility effects.

APPLICATIONS TO OTHER CONFIGURATIONS

Flaps and ailerons may be added to the wing by using an approach somewhat
similar to that of Lan (ref. 2). For the chordwise integration, the interval
from the leading edge of the wing to the flap leading edge is transformed into
$[0,\pi]$ by the "semicircle method", and the interval from the flap leading edge
to the trailing edge is also mapped into $[0,\pi]$ by another "semicircle". The
same technique can also be applied in the spanwise direction.

Application of the present method to tapered and/or swept wings requires
additional considerations. Care must be exercised so that the chordwise vortex
and control points at one spanwise location match those at another spanwise
position in order to evaluate the Cauchy integral properly. These configura-
tions are presently being studied along with non-planar wings.

CONCLUDING REMARKS

A new method is developed for solving the lifting-surface equation for
thin, subsonic wings. The downwash equation is written as Cauchy-type inte-
grals for the chordwise and spanwise directions. They can be interpreted as a
lattice of horseshoe vortices and the positions of the vortices and control
points are determined by the finite sum used to approximate the integrals.
Lan's two-dimensional method is used for the chordwise integral since it pro-
perly accounts for the leading-edge singularity, Cauchy singularity, and the
Kutta condition. For the spanwise integral, Multhopp's interpolation formula is
used in conjunction with the midpoint trapezoidal rule and the theory of
Chebychev polynomials. This method properly accounts for the Cauchy singularity

313

and yields the classical solution to Prandtl's lifting-line equation. The numerical method for evaluating the chordwise and spanwise integrals is much simpler and quicker than other continuous loading methods.

The chordwise and spanwise methods are combined to obtain a continuous loading solution to the lifting-surface equation. The algorithm for the rectangular wing gives results which compare well with other continuous loading methods, but with much smaller computational times. In addition, it converges faster and is more accurate than other vortex lattice methods.

For rectangular wings, the vortex lattice arrangement dictated by the present method differs from the conventional VLM in that the chordwise positions of the vortices and control points do not follow the usual 1/4 - 3/4 rule. There is always a control point at the trailing edge, which allows the Kutta condition to be satisfied, and a control point at the leading edge which yields the leading-edge suction parameter. The spanwise vortices determined by the present method are not uniformly spaced, and the tip vortices are inset from the actual wing tip. This vortex lattice arrangement gives better results than other VLM's for rectangular wings. Other wing planforms require additional considerations, and they are presently being investigated.

REFERENCES

1. Margason, R. J.; and Lamar, J. E.: Vortex-Lattice Fortran Program for Estimating Subsonic Aerodynamic Characteristics of Complex Planforms. NASA TN D-6142, 1971.

2. Lan, C. E.: A Quasi-Vortex Lattice Method in Thin Wing Theory. J. Aircraft, vol. 11, no. 9, Sept. 1974, pp. 518-527.

3. Hough, G. R.: Remarks on Vortex-Lattice Methods. J. Aircraft, vol. 10, no. 5, May 1973, pp. 314-317.

4. Kuethe, A. M.; and Schetzer, J. D.: Foundations of Aerodynamics. John Wiley & Sons, Inc., N. Y., second edition, 1959.

5. Luke, Y. L.: The Special Functions and Their Approximations. Vol. II, Chap. XV, Academic Press, N. Y., 1969.

6. Ashley, Holt; and Landahl, M. T.: Aerodynamics of Wings and Bodies. Addison-Wesley Publishing Co., Inc., Mass., 1965.

7. Scheid, Francis: Theory and Problems of Numerical Analysis. Schaum's Outline Series, McGraw-Hill Book Co., N. Y., 1968.

8. Garner, H. C.; Hewitt, B. L.; and Labrujere, T. E.: Comparison of Three Methods for the Evaluation of Subsonic Lifting Surface Theory. Reports and Memoranda 3597, Aeronautical Research Council, London, England, June 1968.

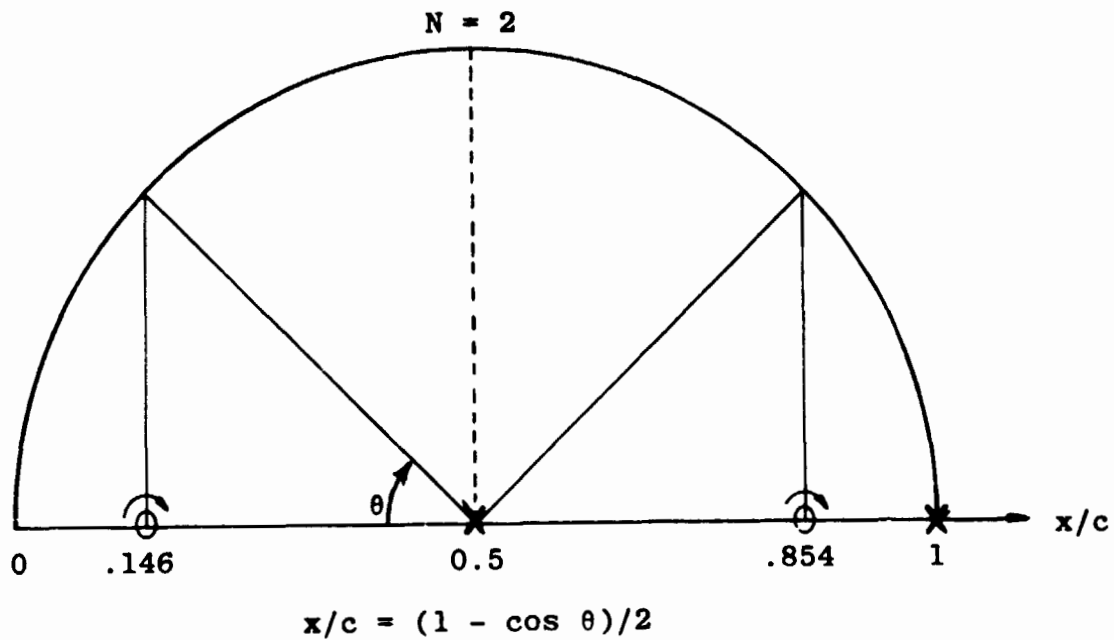TABLE 1. RESULTS FOR RECTANGULAR PLANFORM
A = 2

	Present N=4, M=16	NLR (ref. 8) N=4, M=16	Lan (ref. 2) N=8, M=30	VLM (ref. 1) N=6, M=40	Wagner from ref. 2
Overall Values					
C_{L_α}	2.4732	2.4744	2.4707	2.5239	2.4778
$-C_{M_\alpha}$	0.5187	0.5182	0.5173	0.5334	0.5180
X_{ac}/C	0.2097	0.2094	0.2094	0.2113	0.2091
$1/e$	1.0007	1.0007	1.0050	1.0018	1.0005
$1/e_{nf}$	0.9951	1.0108	1.0022	0.9764	1.0172

Values of c_ℓ/C_L

2y/b	Present	NLR
0	1.2543	1.2543
0.1951	1.2331	1.2331
0.3827	1.1692	1.1692
0.5556	1.0625	1.0625
0..071	0.9137	0.9137
0.8315	0.7257	0.7257
0.9239	0.5045	0.5044
0.9808	0.2588	0.2587

Values of x_{ac}/c

2y/b	Present	NLR
0	0.2200	0.2199
0.1951	0.2187	0.2187
0.3827	0.2150	0.2149
0.5556	0.2087	0.2085
0.7071	0.1999	0.1996
0.8315	0.1896	0.1886
0.9239	0.1798	0.1773
0.9808	0.1731	0.1685

Figure 1.- Lan's vortex arrangement for airfoils.

The figure shows a semicircle with:

$$N = 2$$

along the horizontal axis labeled x/c with points at 0, $.146$, 0.5, $.854$, 1, and the angle θ measured from 0.5.

$$x/c = (1 - \cos \theta)/2$$

O Vortex Position: $\theta_k = \dfrac{(2k - 1)\pi}{2N}$ $(k = 1, \ldots, N)$

X Control Points : $\theta_i = \dfrac{i\pi}{N}$ $(i = 1, \ldots, N)$
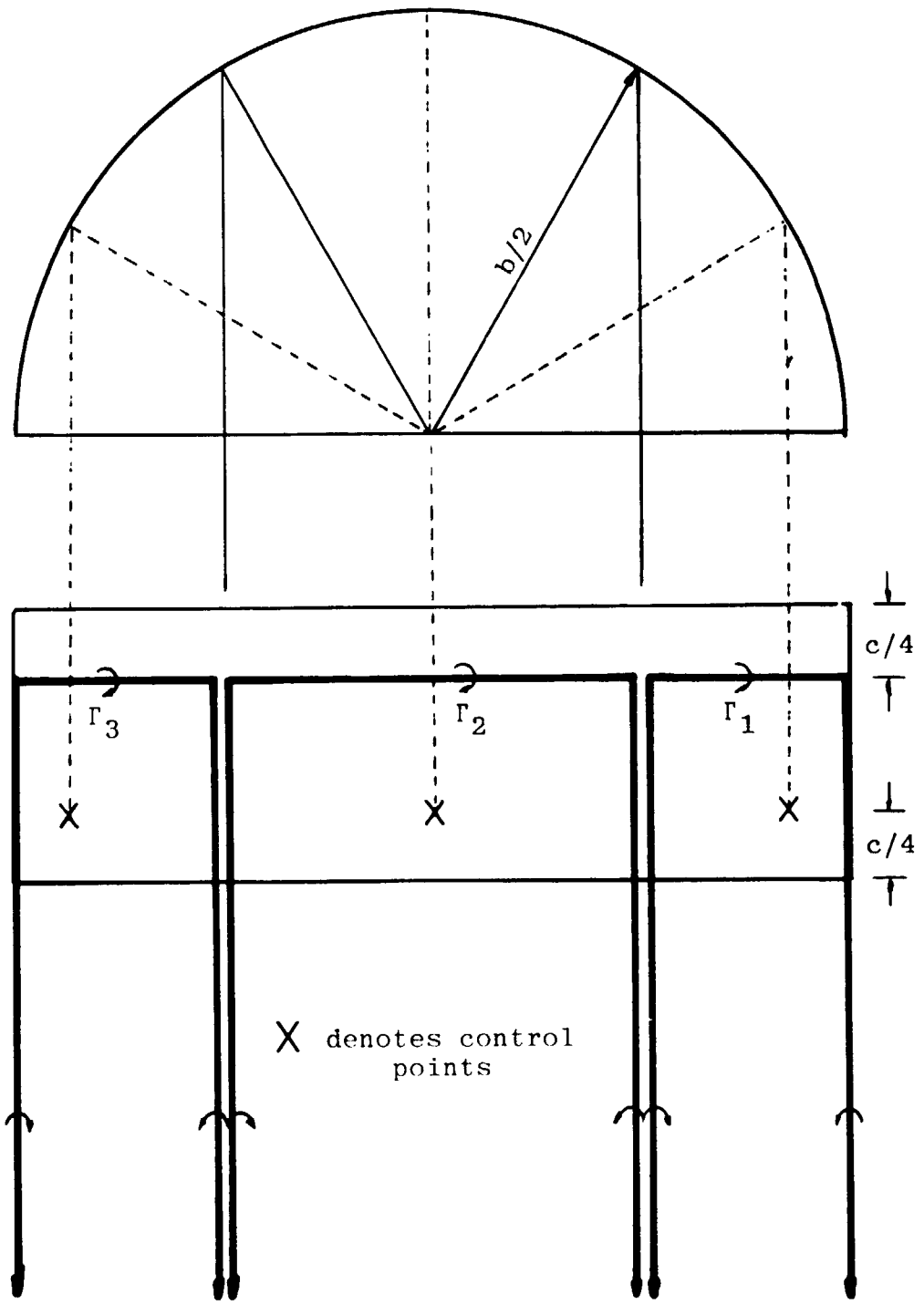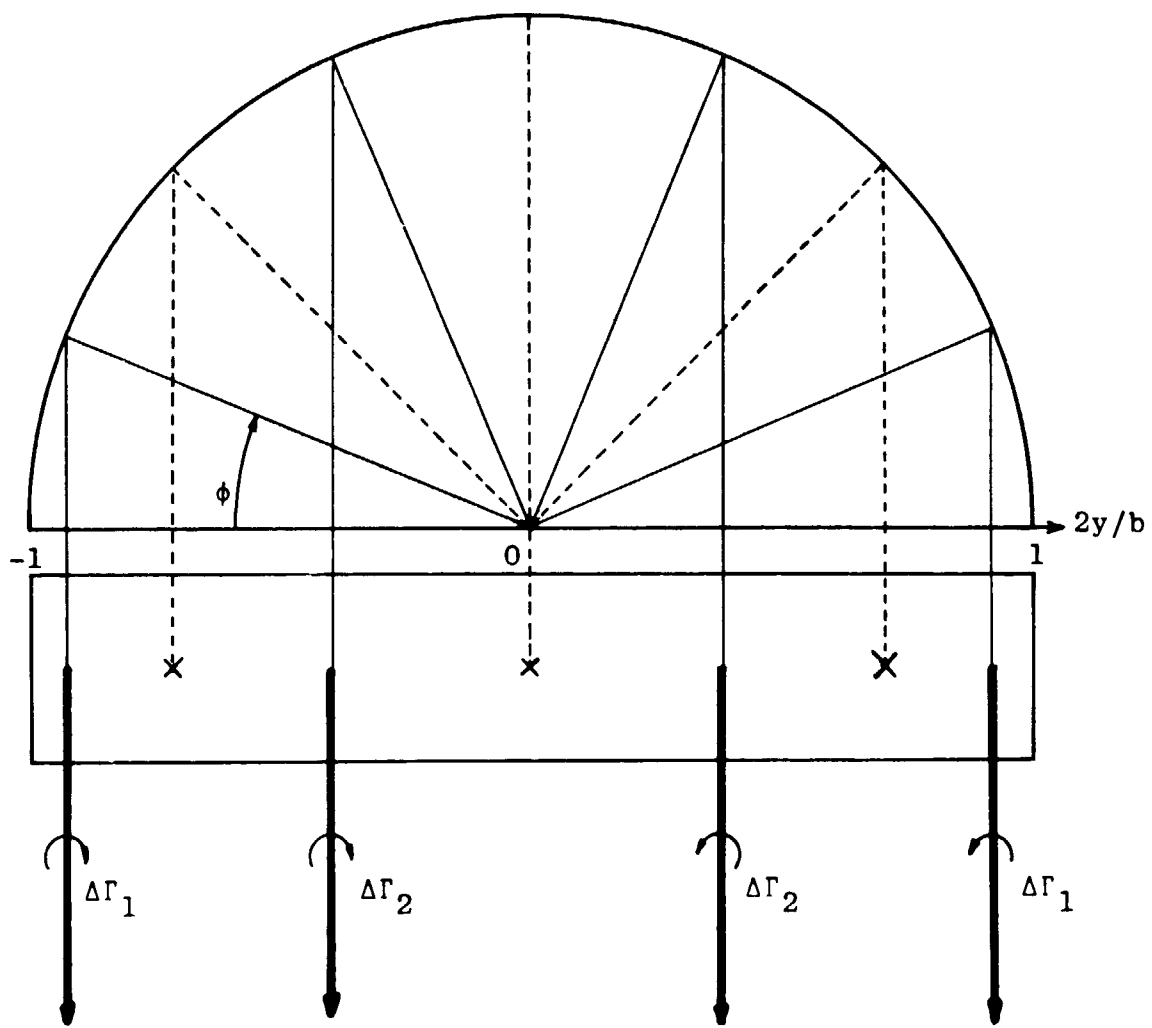
Figure 2.- Conventional arrangement of vortex lattice (illustrated for N = 1, M = 4).

X = Spanwise Control Points   Rectangular Wing for M = 4

Figure 3.- Arrangement of trailing vortices for Prandtl's
lifting-line equation.
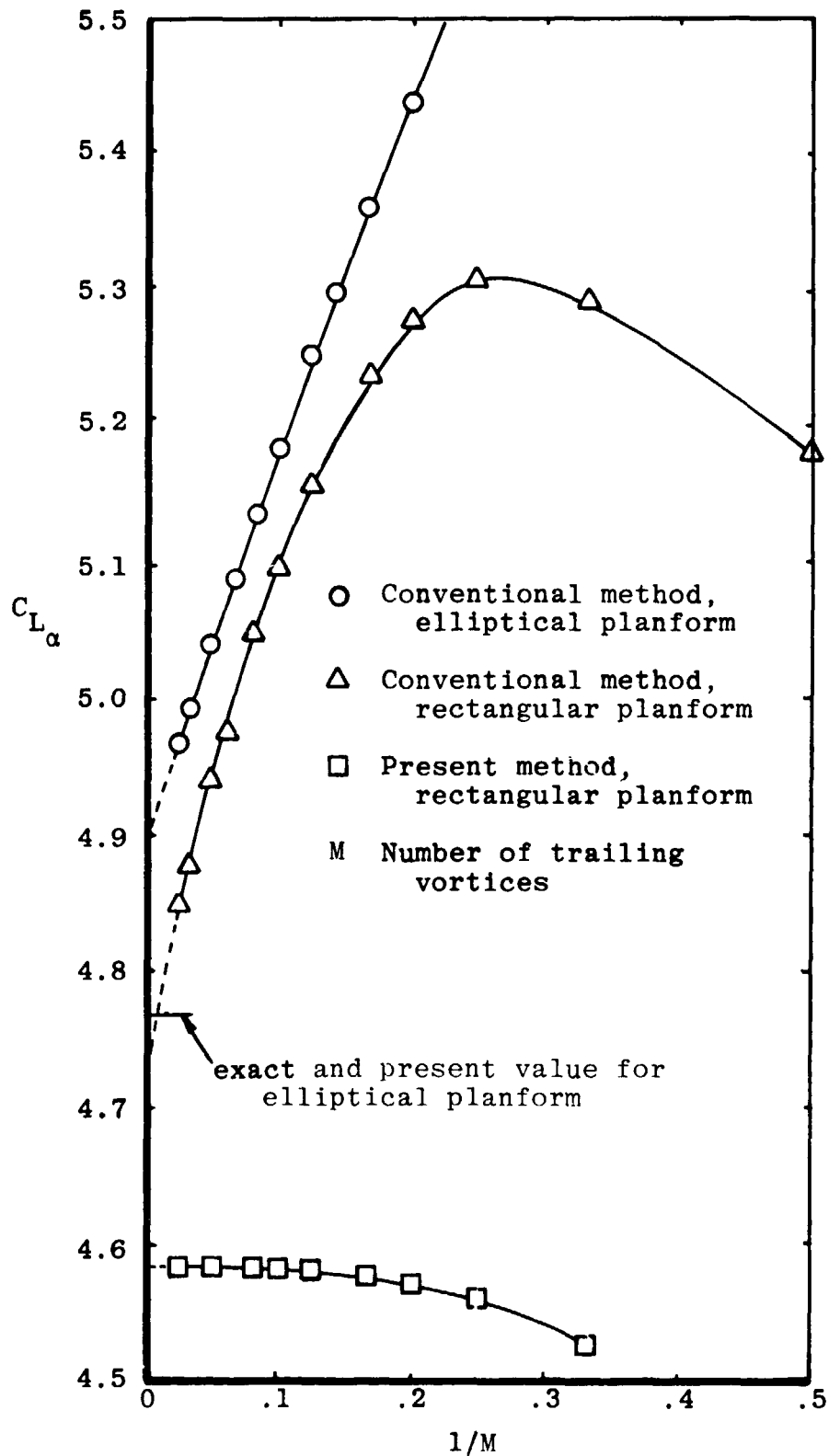
Figure 4.- Effect of number of trailing vortices on C_{L_α} from Prandtl's lifting-line theory, $A = 2\pi$.
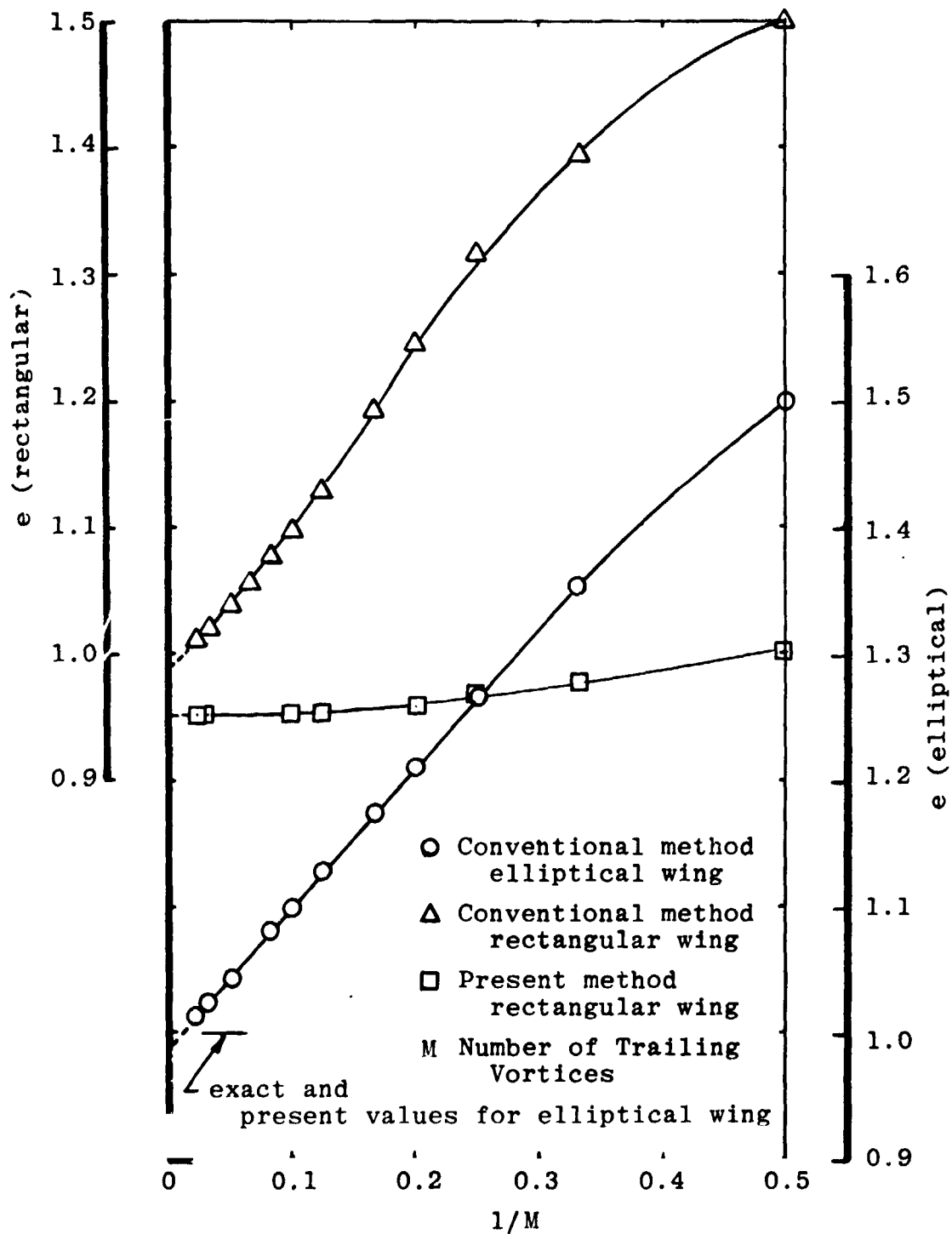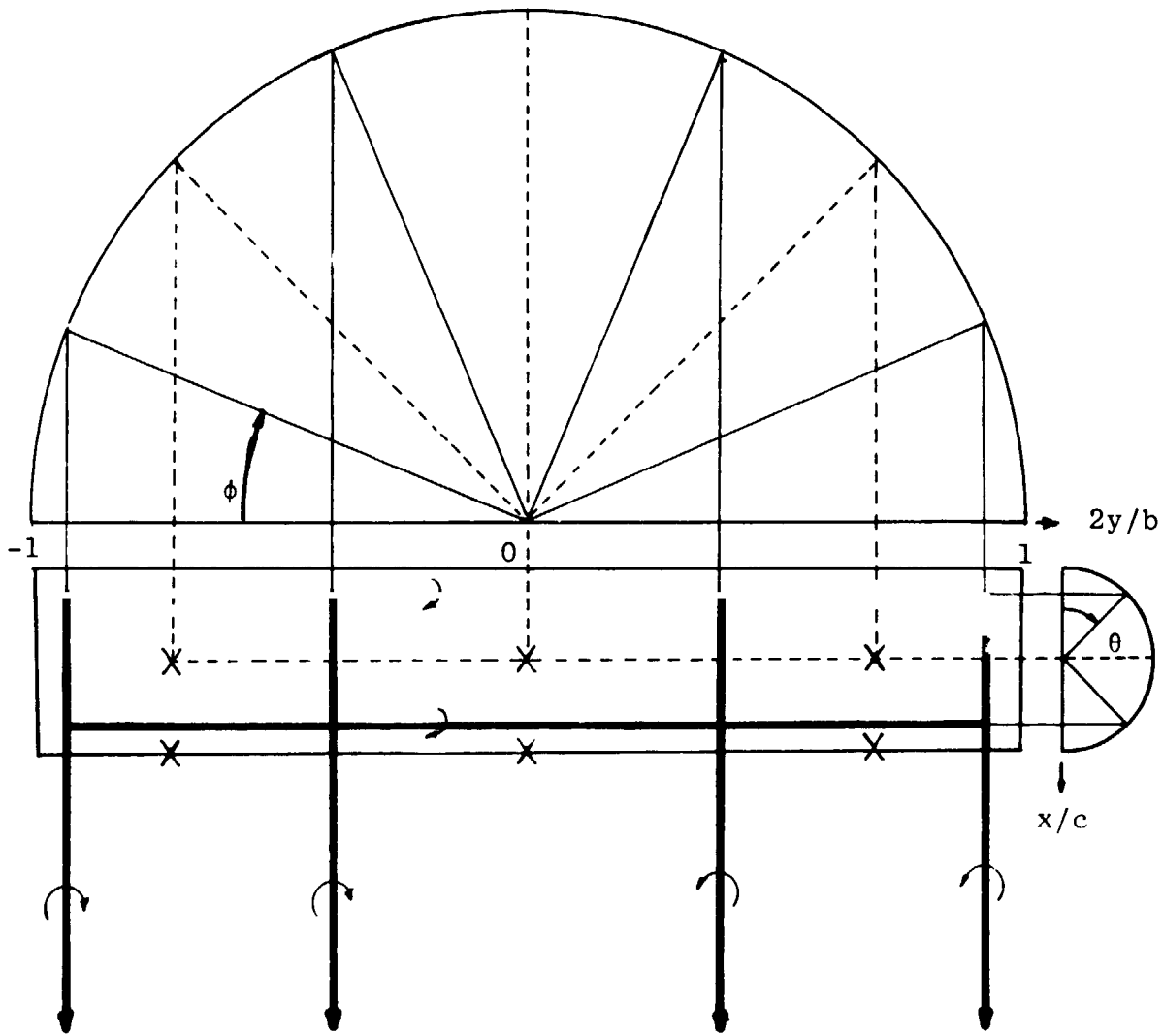
Figure 5.- Effect of number of trailing vortices on induced
drag from Prandtl's lifting-line theory, $A = 2\pi$.

Figure 5.- Effect of number of trailing vortices on induced
drag from Prandtl's lifting-line theory, $A = 2\pi$.

X = Control Points

Rectangular Wing for

N = 2, M = 4

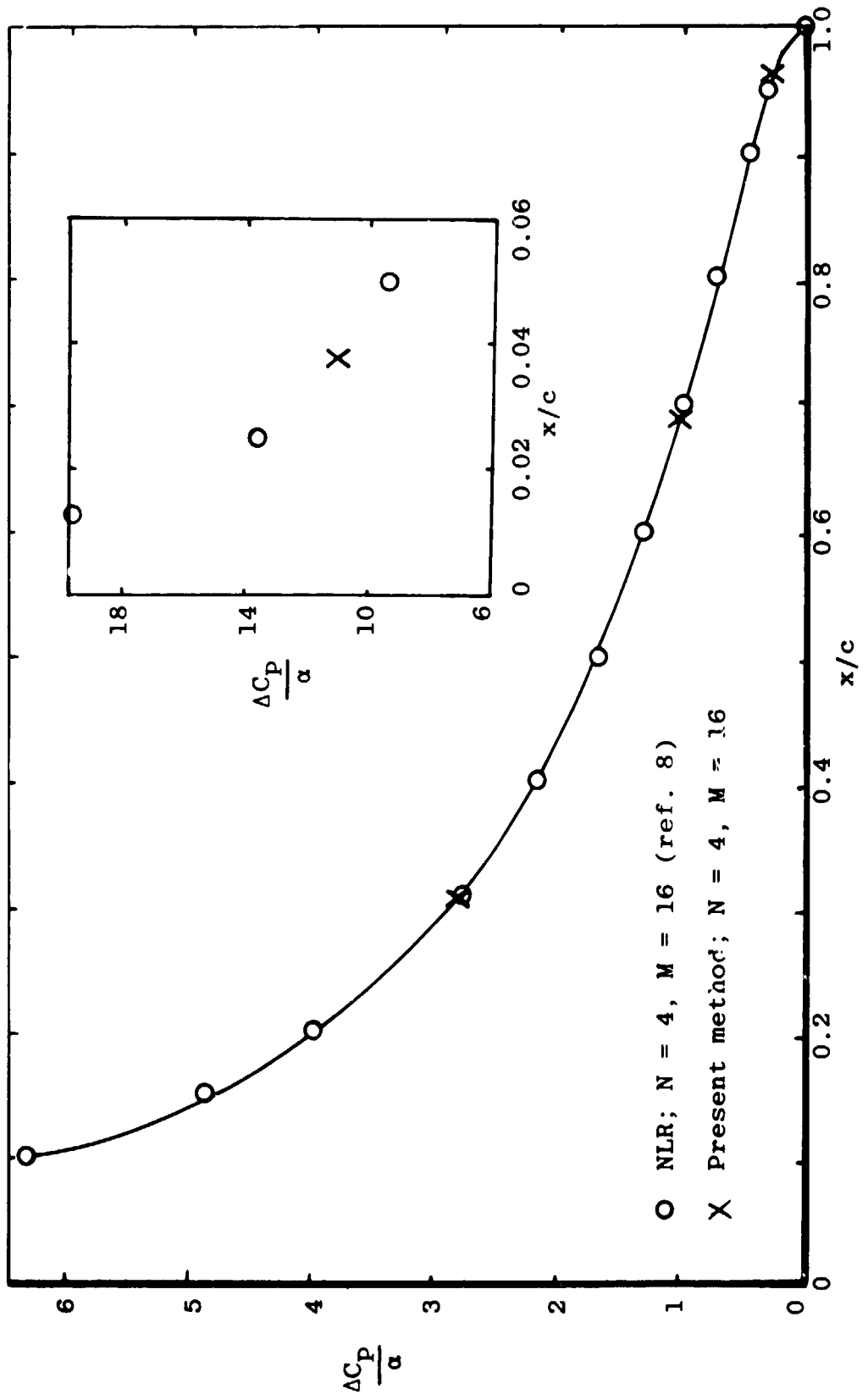Figure 6.- Arrangement of vortex lattice for lifting-surface equation.

Figure 7.- Chordwise loading at midspan on rectangular wing, A = 2.

O NLR; N = 4, M = 16 (ref. 8)

X Present method; N = 4, M = 16

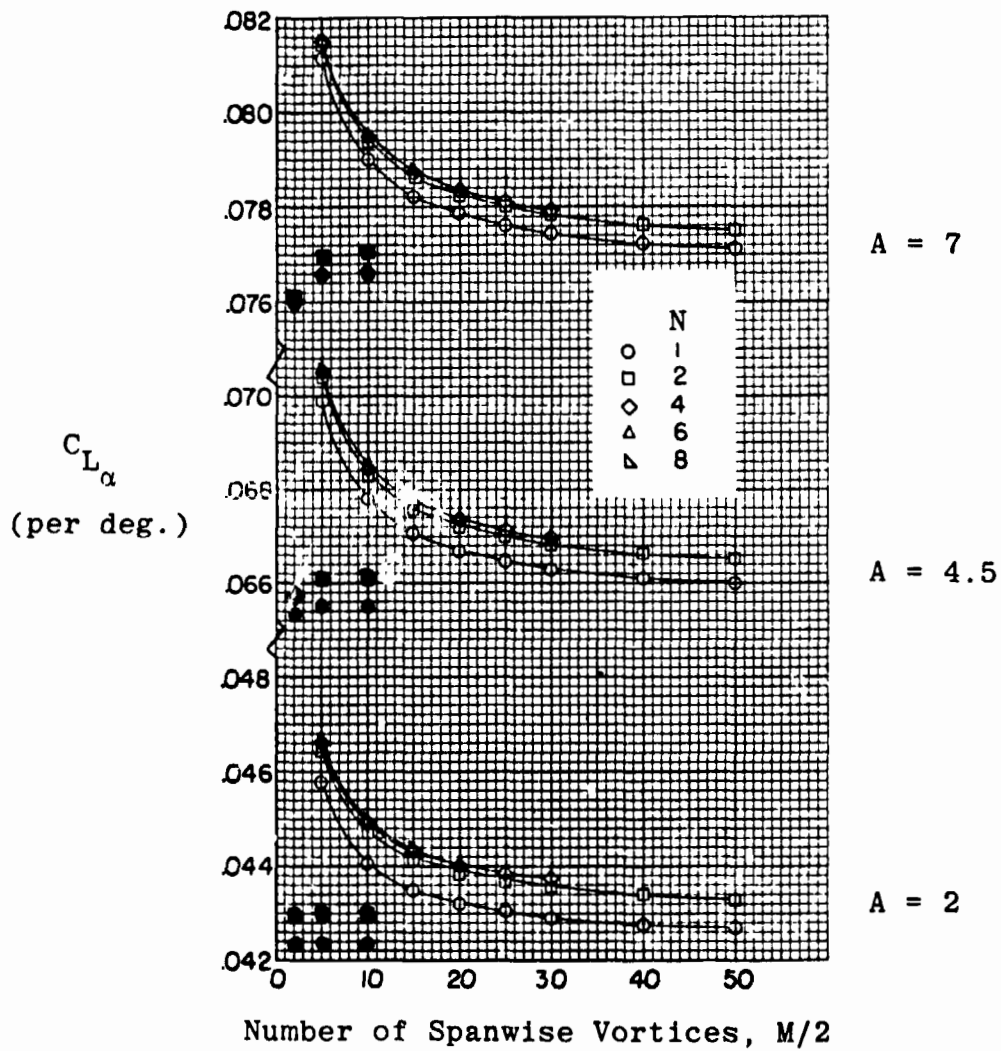Open Symbols - VLM (ref. 1)

Solid Symbols - Present Method

Figure 8.- Effect of vortex-lattice arrangement for
rectangular planforms.